

Dynamical quantum phase transitions

Ralf Schützhold*

*Institut für Theoretische Physik, Technische Universität Dresden, D-01062 Dresden, Germany
Fachbereich Physik, Universität Duisburg-Essen, D-47048 Duisburg, Germany*

A sweep through a quantum phase transition by means of a time-dependent external parameter (e.g., pressure) entails non-equilibrium phenomena associated with a break-down of adiabaticity: At the critical point, the energy gap vanishes and the response time diverges (in the thermodynamic limit). Consequently, the external time-dependence inevitably drives the system out of equilibrium, i.e., away from the ground state, if we assume zero temperature initially. In this way, the initial quantum fluctuations can be drastically amplified and may become observable – especially for symmetry-breaking (restoring) transitions. By means of several examples, possible effects of these amplified quantum fluctuations are studied and universal features (such as freezing) are discussed.

I. MOTIVATION

In many cases, the properties of the ground state (or, at finite temperatures, the thermal equilibrium state) are sufficient for understanding the behavior of a given condensed-matter system. In many other scenarios, however, the actual quantum state shows significant deviations from the ground state and non-equilibrium phenomena have to be taken into account. Even if the system starts near the (initial) ground state, it may depart during the evolution – for example, due to an external time-dependence.

For example, let us consider an explicitly time-dependent Hamiltonian with a discrete (non-degenerate) spectrum $H(t)|\psi_n(t)\rangle = E_n(t)|\psi_n(t)\rangle$. After inserting this instantaneous eigenvector expansion into the Schrödinger equation and some approximations, one obtains the adiabatic expansion

$$|\psi(t)\rangle \approx |\psi_0(t)\rangle + \sum_{n>0} \frac{\langle \psi_n | \dot{H} | \psi_0 \rangle}{(E_n - E_0)^2} e^{i\varphi_n} |\psi_n(t)\rangle. \quad (1)$$

I.e., if the system started in its ground state $|\psi_0(t_0)\rangle$, its actual quantum state $|\psi(t)\rangle$ will remain near [1] the instantaneous ground state $|\psi_0(t)\rangle$ if the non-adiabatic corrections are small, i.e., if $\langle \psi_n | \dot{H} | \psi_0 \rangle \ll (E_n - E_0)^2$. The latter condition compares the rapidity of the external time dependence \dot{H} with the internal response times given by the energy level spacings $\Delta E_n = E_n - E_0$. If the response time of the system is short enough such that it can adapt to the external variation, it will stay near the ground state – if the externally imposed change is too fast, however, the system cannot respond and will depart from the instantaneous ground state $|\psi_0(t)\rangle$, leading to the creation of excitations $|\psi_{n>0}\rangle$, e.g., quasi-particles.

This observation directly indicates the close ties between (quantum) phase transitions [2] and non-equilibrium phenomena: At the critical point, at least some of the energy levels converge $\Delta E_n = (E_n - E_0) \downarrow 0$ and hence the associated response times diverge $\Delta E \Delta t \sim \hbar$, which makes it very easy to depart from equilibrium, even for very slow external time dependences \dot{H} , see, e.g., [3–5] Of course, the resulting non-

equilibrium phenomena do not just depend on the energy levels $\Delta E_n = (E_n - E_0)$, the matrix elements $\langle \psi_n | \dot{H} | \psi_0 \rangle$ are also very important.

II. FIRST EXAMPLE

Let us start by considering a very simple example: a homogeneous two-component Bose-Einstein condensate [6]. In the dilute-gas limit, the Hamiltonian density reads

$$\mathcal{H} = \sum_{ab} \hat{\Psi}_a^\dagger \left(-\frac{\nabla^2}{2m} + \frac{g_{ab}}{2} \hat{\Psi}_b^\dagger \hat{\Psi}_b \right) \hat{\Psi}_a, \quad (2)$$

where $\hat{\Psi}_a = (\hat{\Psi}_1, \hat{\Psi}_2)$ denote the field operators of the two components, m the mass of the condensed particles, and g_{ab} the coupling matrix in the s -scattering approximation. Using the mean-field approximation and Madelung spilt $\hat{\Psi}_a \approx \Psi_a = \sqrt{\rho_a} \exp(i\Phi_a)$ with the densities $\rho_a > 0$ and the phases Φ_a , we obtain two decoupled Goldstone modes due to the broken $U(1) \otimes U(1)$ symmetry $\Phi_\pm = (\delta\Phi_1 \pm \delta\Phi_2)/\sqrt{2}$. The hard density mode Φ_+ corresponds to variations of the total density $\rho = \rho_1 + \rho_2$ while the soft spin mode Φ_- is associated to the density difference $\rho_1 - \rho_2$. The propagation velocities of the two modes are given by the eigenvalues $g_\pm = (g_{11} + g_{22})^2/4 \pm \sqrt{(g_{11} - g_{22})^2/4 + g_{12}^2}$ of the coupling matrix g_{ab} . Depending on the relation between the inter-component repulsion $g_{12} = g_{21} > 0$ and the intra-component couplings $g_{11}, g_{22} > 0$, there is a phase transition when g_- changes its sign. If the repulsion within the same component g_{11}, g_{22} dominates, the condensate will be in the homogeneous mixed state $\rho_1 = \rho_2$. In case the particles of different components repel each other more strongly, the inhomogeneous phase separated state (either $\rho_1 = 0$ or $\rho_2 = 0$) will be energetically favorable, see Fig. 1.

Now, let us study the sweep through this phase transition by means of a time-dependent $g_{12}(t)$ starting in the mixed state. The hard density modes Φ_+ will basically remain unaffected by the transition, but the spin modes Φ_- become arbitrarily soft when approaching the critical point $g_- = 0$ and finally become unstable on the other side. Hence these modes are the most interesting ones. In such a sweep, there will be four major stages:

*Electronic address: ralf.schuetzhold@uni-due.de

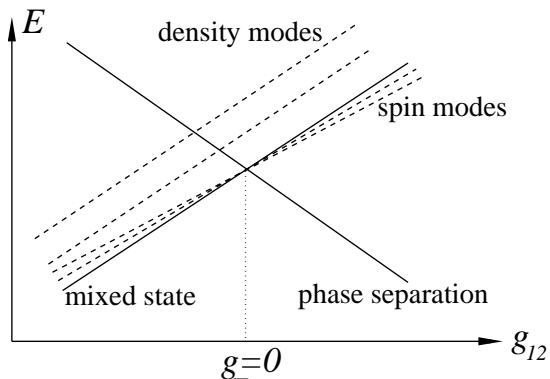


FIG. 1: Sketch of the level structure from Eq. (2) near the critical point $g_- = 0$ separating the mixed condensate from the phase separated state. The two solid lines denote these two competing ground states which cross at $g_- = 0$ and the quasi-particle excitations are depicted by dashed lines.

- **cooling** Since approaching the critical point implies a reduction of the quasi-particle energies $\Delta E_n = E_n - E_0$ of the spin modes, their temperature (if non-zero initially) will drop as long as we are still approximately in equilibrium (i.e., adiabatic).
- **freezing** Close enough to the critical point, however, the spin modes become too soft, i.e., slow, and thus cannot adapt to the externally imposed variation $g_{12}(t)$ anymore, i.e., they freeze.
- **squeezing** Even if we started in the initial ground state, this freezing of the modes implies a squeezing (and thus amplification) of the quantum fluctuations due to the breakdown of adiabaticity, cf. Eq. (1) and Fig. 2.
- **re-heating** Finally, far enough on the other side of the phase transition, the system starts to “realize” that it is not in its true ground state and the spin modes start to grow exponentially – with the frozen and amplified quantum fluctuations as initial seeds.

Interestingly, this sequence: cooling \rightarrow freezing \rightarrow squeezing \rightarrow re-heating exhibits striking similarities to cosmic inflation. Indeed, one might speculate whether cosmic inflation was not a real expansion of the universe over many orders of magnitude, but instead represent our distorted view of an early cosmic phase transition [7].

III. HORIZON ANALOGUE

Let us study the general behavior mentioned in the previous Section in some more detail. To this end, we have to consider the equation of motion for the spin modes. Of course, we could derive it directly from the original Hamiltonian (2). However, for the sake of universality, let us base our discussion on general arguments instead. Assuming that the spin modes can be described by a linearized low-energy effective

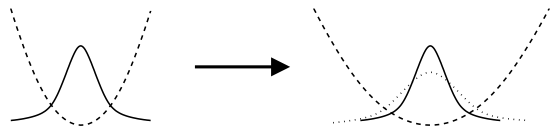


FIG. 2: Schematic of the squeezing (amplification) of the quantum fluctuations. Each (linearized) quasi-particle mode corresponds to a harmonic oscillator, whose potential is depicted as a dashed curve. Initially (left picture), the mode is in its ground state (solid curve). Approaching the critical point, the modes become softer and hence the potential gets more shallow (right picture). As long as this happens slow enough [cf. Eq. (1)], the quantum state evolves adiabatically and stays near the instantaneous ground state (dotted curve). After freezing, however, the modes cannot adapt to this change anymore and their quantum state (solid curve in right picture) deviates from the ground state (dotted curve). In view of the linearity of the equations of motion, the quantum state evolves into a squeezed state (e.g., the wave function is still Gaussian). This squeezing effect becomes even more pronounced if the quadratic potential turns over, as in Fig. 9. The direction in which the quantum fluctuations will be amplified depends on the system under consideration. For a symmetry-breaking transition (where the potential turns over, cf. Fig. 5), for example, the quantum fluctuations typically grow in the direction of symmetry-breaking.

action, we write down the most general form for scalar Goldstone modes in a homogeneous and isotropic medium [7]

$$\mathcal{L}_{\text{eff}} = \frac{1}{2} \left(\frac{1}{\alpha[g_-(t)]} \dot{\Phi}_-^2 - \beta[g_-(t)] (\nabla \Phi_-)^2 \right), \quad (3)$$

where the two remaining factors α and β are functions of the external parameter $g_-(t)$ and have to be determined from the underlying system. Accordingly, the effective energy (Hamiltonian) density of these Goldstone modes reads

$$\mathcal{H}_{\text{eff}} = \frac{1}{2} \left(\alpha[g(t)] \Pi^2 + \beta[g(t)] (\nabla \Phi)^2 \right). \quad (4)$$

Before the transition, the spin modes are stable and hence α and β must be positive. After the transition, however, the spin modes become unstable and thus at least one of the two parameters has to change its sign, i.e., it must vanish at the critical point. As a result, the propagation velocity $c^2 = \alpha\beta$ must also go to zero when approaching the transition, which precisely reflects the fact that the spin modes become infinitely soft.

The consequence of such an evanescent propagation velocity $c(t)$ can nicely be explained by the analogy to gravity/cosmology: For a constant speed $dc/dt = 0$, quasi-particle excitations may propagate arbitrarily far through the sample (in the absence of damping etc.) if we wait long enough. If $c(t)$ decreases sufficiently fast, however, the excitations may not travel infinitely far – even if one waits long enough and takes an infinite time to reach the critical point – but merely a finite distance, which is an exact analogue of a cosmic horizon

$$\Delta r(t) = \int_t^\infty dt' c(t'). \quad (5)$$

The horizon size $\Delta r(t)$ corresponds to the maximum distance covered by quasi-particles starting at time t and hence measures the range of causal connection [8]. Of course, in a real experiment, the critical point is crossed after a finite time, which should then be used as the upper limit (with the physics conclusions remaining unchanged).

Two points at distances larger than the horizon $\Delta r(t)$ can no longer exchange information or energy, i.e., the horizon describes a dynamical loss of causal connection. Since maintaining equilibrium requires causal connections between all points of the sample (e.g., in order to equilibrate local density variations), this loss of causal connection indicates the departure from equilibrium and the breakdown of adiabaticity. As mentioned before, this typically entails an amplification of the quantum fluctuations, which can be understood in the following way: Since the analogue horizon shrinks steadily

$$\frac{d}{dt}\Delta r(t) = \frac{d}{dt} \int_t^\infty dt' c(t') = -c(t), \quad (6)$$

it will engulf every wavelength λ after a given time. Therefore, all modes λ will pass through the three main stages of their evolution:

- **oscillation** Initially $\lambda \ll \Delta r(t)$, the modes do not notice the horizon and oscillate almost freely (though with a decreasing frequency, cf. the cooling in the previous Section).
- **horizon crossing** At some point of time, the horizon closes in $\lambda \sim \Delta r(t)$ and inhibits further oscillations because crest and trough of a wave are separated by the horizon and hence cannot exchange energy anymore.
- **freezing & squeezing** After that, the modes are frozen and cannot respond to the external change anymore, i.e., the initial Gaussian ground state will turn into a squeezed state representing the amplification of the quantum fluctuations, cf. Fig. 2.

According to our standard model of cosmology, precisely the same mechanism occurred in the early universe (during inflation) and is responsible for the generation of the seeds for structure formation out of the initial quantum vacuum fluctuations. Traces of these amplified quantum vacuum fluctuations can still be observed today in the anisotropies of the cosmic microwave background radiation.

IV. UNIVERSALITY?

Now, after having studied this specific example, one is lead to the question of how universal these phenomena really are. In order to study this point, let us have a look at the effective energy landscape in terms of the order parameter $x = \rho_1/(\rho_1 + \rho_2)$. It is restricted according to $0 \leq x \leq 1$ with the boundary values representing the phase separated region while the mixed state is given by $x = 1/2$. Inserting this ansatz into the Hamiltonian (2), the relevant part of the energy

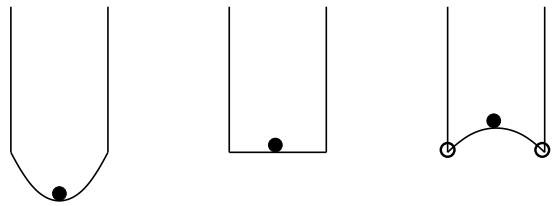


FIG. 3: Sketch of the energy landscape associated to Eq. (2). The filled black dot denotes the initial ground state (mixed condensate) and the hollow dots correspond to the final ground states (phase separation). In view of the jump in the ground state structure, the phase transition is of first order – though it is a somewhat untypical example, since the energy landscape becomes flat (in the relevant direction) at the critical point (middle panel).

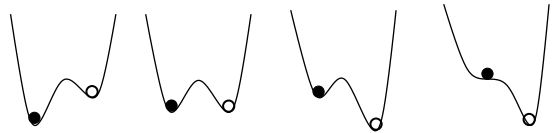


FIG. 4: Sketch of the energy landscape associated to a typical first-order phase transition. Again the filled/hollow black dot denotes the initial/final ground state. In this case, the vicinity of the initial ground state remains (locally) stable at the critical point (second panel from the left) and the linearized quasi-particle modes do not become arbitrarily soft at this stage. Typically, this happens much later, at the point of instability of the initial ground state (right panel).

functional reads $g_-(x - 1/2)^2$, which is plotted in Fig. 3. Even though the phase transition is of first order (on the mean-field level), it is a somewhat untypical example, because the energy landscape becomes flat at the critical point. Therefore, adding a small non-linearity such as $(x - 1/2)^4$ would turn it into a transition of second order.

In contrast, the energy landscape of a typical first-order transition is sketched in Fig. 4. In this case, the vicinity of the initial ground state remains stable even after the transition and there is no local linearized mode connecting the two competing vacua before one reaches the point of instability, cf. Fig. 4, right panel. Therefore, the previous arguments (softening of modes etc.) do not apply to the critical point, but they could be applied to the point of instability (which occurs later).

The aforementioned instability of the transition in Fig. 3 towards the transformation into a second-order transition already suggests that the phenomena discussed in the previous Sections could also be relevant for transitions of higher order. Fig. 5 depicts the energy landscape of a typical symmetry-breaking second-order phase transition. As suggested by this picture, there will be some modes which become arbitrarily soft at the critical point and unstable afterwards, i.e., during the sweep through such a transition, one generally reproduces the sequence: cooling \rightarrow freezing \rightarrow squeezing \rightarrow re-heating. Transversing the critical point in the opposite direction (i.e., a symmetry-restoring transition), there are still modes which become arbitrarily soft – but they do not necessarily become unstable. Consequently, the shorter sequence: cooling \rightarrow freezing \rightarrow squeezing does also apply here, but the re-heating

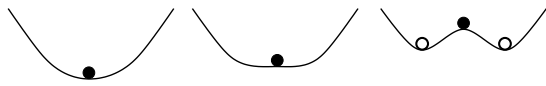


FIG. 5: Sketch of the energy landscape associated to a typical symmetry-breaking second-order transition. At the critical point (middle panel), the local curvature in the vicinity of the initial ground state (filled dot) changes its sign and hence the associated quasi-particle modes become arbitrarily soft at the transition and turn unstable afterwards. The time-reversed sweep corresponds to a symmetry-restoring transition. In this case, the ground state (hollow dot) does not become unstable, but still the associated quasi-particle modes become arbitrarily soft at the transition.

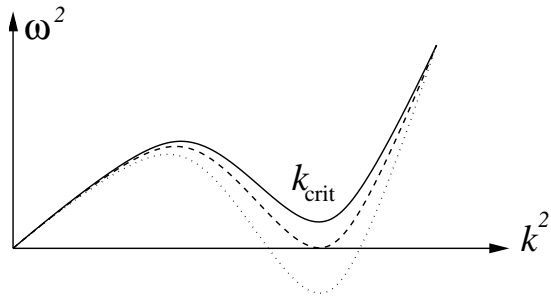


FIG. 6: Typical evolution of the dispersion relation where the instability occurs at a finite wavenumber k_{crit} . Before the transition (solid curve), the frequencies are non-negative. At the critical point (dashed curve), the “roton” dip touches the axis and afterwards, the modes in the vicinity of k_{crit} start to grow (dotted curve).

part requires further considerations.

Of course, having established that some modes become arbitrarily soft when approaching the critical point does not mean that they behave like the spin modes in Eq. (3). For the example in Sec. II, the typical length scale of the amplified quantum fluctuations was set by the horizon size and thus the sweep rate dc/dt . This is not always the case. In order to explore the different possibilities, let us study quasi-particle modes which become arbitrarily soft when approaching the critical point (and unstable afterwards). Their relevant features should be encoded in the quasi-particle dispersion relation $\omega(\vec{k})$. Assuming invariance under time-reversal and reflection as well as (spatial) rotations[26], it simplifies to $\omega^2(\vec{k}^2)$. The critical point then occurs when $\omega^2(\vec{k}^2)$ starts to dive below the vertical axis. This could happen at non-zero k , see Fig. 6, or at zero k . In the latter case, we may employ a Taylor (i.e., low-energy) expansion similar to Eq. (3)

$$\omega^2(\vec{k}^2) = m^2 + c^2\vec{k}^2 + \mathcal{O}(\vec{k}^4). \quad (7)$$

Thus there are two options for an instability: either m^2 changes its sign, see Fig. 7, or c^2 changes its sign while $m = 0$, see Fig. 8. Note that the case of c^2 changing its sign in the presence of a positive m^2 would bring us back to the case in Fig. 6.

An example for the scenario in Fig. 6 is the extended Bose-Hubbard model (cf. Sec. VI) where the dispersion relation may possess a “roton” dip which dives below the vertical axis at the superfluid-supersolid phase transition. In this case, the

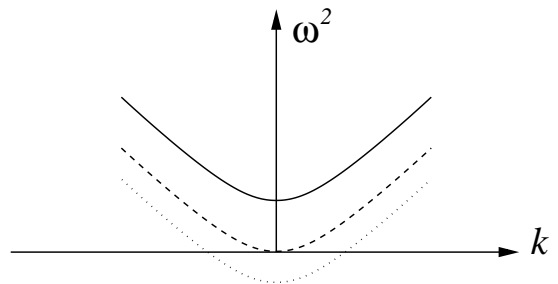


FIG. 7: Typical evolution of the dispersion relation where the instability occurs at $k = 0$ since the quasi-particle gap – i.e., their effective mass m^2 in Eq. (7) – changes sign.

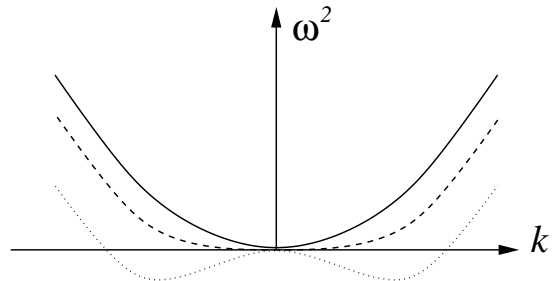


FIG. 8: Typical evolution of the dispersion relation where the instability occurs at $k = 0$ since the quasi-particle stiffness c^2 of the Goldstone modes changes sign, cf. (3).

typical length scale of the amplified quantum fluctuations is naturally set by the characteristic wavenumber k_{crit} at the “roton” dip, which determines the period of the supersolid order and is independent of the sweep rate etc. However, spatial modulations around this wavenumber k_{crit} (which could induce defects in the supersolid crystal, for example) may depend on the sweep rate.

The instability at small k sketched in Fig. 7 occurs in the example discussed in Sec. VII. In contrast to Fig. 6, the characteristic length scale cannot be read off the critical dispersion relation (dashed curve) in general. Instead, it is set by the sweep rate and/or the final state[27], depending on the system parameters. For the experiment [13] discussed in Sec. VII, the final state determines the characteristic length scale. In other regions of parameter space (e.g., with a much slower quench), however, the sweep rate may yield the dominant contribution. In this situation, a quantum version of the Kibble-Zurek [14, 15] scaling arguments [16] may be applied: The time-dependent correlation length $\xi(t) \propto 1/m(t)$ is cut off at the time \tilde{t} when adiabaticity breaks down, i.e., $\tilde{t} \simeq t_{\text{response}}(\tilde{t}) \propto 1/\Delta E(\tilde{t})$. This saturated correlation length $\tilde{\xi} = \xi(\tilde{t})$ then determines the typical distance of the topological defects.

Finally, the case of Goldstone modes (which become unstable upon crossing the transition) is sketched in Fig. 8. For example, the system discussed in Sec. II falls into this category. Note that Fig. 3 describes the behavior of that system under large but homogeneous (i.e., $k = 0$) displacements, whereas the dispersion relation in Fig. 8 corresponds to small (lin-

earized) inhomogeneous displacements with various k . In this case, the concept of a horizon analogue sketched in Sec. III can be applied. In the vicinity of the critical point (dashed line in Fig. 8), the time-dependent horizon size in Eq. (5) determines the spectrum [7] and the typical length scales of the amplified quantum fluctuations, but after the transition (dotted line in Fig. 8), the final state typically induces an additional length scale corresponding to the fastest growth of the modes (negative minima of dispersion curve). Note that the Kibble-Zurek scaling arguments sketched above do not apply in this situation: Modes with different k cross the horizon in Eq. (5) and thus freeze (i.e., become non-adiabatic) at different times – hence, there is no unique time \tilde{t} and consequently no saturated correlation length $\tilde{\xi} = \xi(\tilde{t})$.

V. BOSE-HUBBARD MODEL

Now, after having discussed some general aspects, let us turn to a few explicit examples. A prototypical example [2] for a second-order phase transition is the Bose-Hubbard model

$$\hat{H} = J(t) \sum_{\alpha\beta} M_{\alpha\beta} \hat{a}_\alpha^\dagger \hat{a}_\beta + \frac{U}{2} \sum_{\alpha} (\hat{a}_\alpha^\dagger)^2 \hat{a}_\alpha^2. \quad (8)$$

As usual, $\hat{a}_\alpha^\dagger, \hat{a}_\beta$ are the (bosonic) creation/annihilation operators for the lattice sites α and β , respectively. Hence, the first term describes hopping between the lattice sites α and β , where the lattice structure (e.g., cubic) is encoded in the matrix $M_{\alpha\beta}$ and the tunneling rate $J(t)$ is chosen to be time-dependent. The second term describes the fact that two bosons repel each other if they are on the same lattice site, where U denotes the associated energy penalty. For integer filling $n = \langle \hat{a}_\alpha^\dagger \hat{a}_\alpha \rangle = \langle \hat{n}_\alpha \rangle \in \mathbb{N}$, the system undergoes a second-order quantum phase transition[28] at a critical value of the hopping rate $J_{\text{crit}} = \mathcal{O}(U/n)$. For $J \gg U/n$, the first term dominates and the bosons can move freely on the lattice, which corresponds to the superfluid phase

$$J \gg U/n \rightsquigarrow |\Psi\rangle_{\text{sf}} \propto \left(\sum_{\alpha} \hat{a}_\alpha^\dagger \right)^N |0\rangle, \quad (9)$$

where $N = \sum_{\alpha} n$ is the total number of bosons on the lattice. In the opposite limit $J \ll U/n$, the second term dominates and causes the particles to lock in the lattice sites, i.e., they are not free to move across the lattice anymore. Hence this phase is called the Mott insulator state

$$J \ll U/n \rightsquigarrow |\Psi\rangle_{\text{Mott}} \propto \bigotimes_{\alpha} (\hat{a}_\alpha^\dagger)^n |0\rangle. \quad (10)$$

In the Mott insulator phase, the ground state is separated by a finite gap from the other excited states. The superfluid state, on the other hand, is associated to a certain phase and thus breaks the $U(1)$ symmetry $\hat{a}_\alpha \rightarrow e^{i\varphi} \hat{a}_\alpha$ of the Hamiltonian (8). As a result, this state supports gap-less Goldstone modes, which are the lattice phonons.

Now, let us consider the following scenario: starting deep in the superfluid phase $J \gg U/n$, we decrease the hopping rate $J(t)$ and thereby sweep through the superfluid-Mott phase

transition far into the Mott regime $J \ll U/n$. If we did this infinitely slowly, we would end up in the Mott state (10). A very rapid sweep, on the other hand, would leave the system no time to respond and thus it would stay in the initial coherent state (9). For a finite sweep velocity dJ/dt , one would expect to end up somewhere in between the two states. A good marker for distinguishing the two regimes is the (final) number variance $\Delta^2(n_\alpha) = \langle \hat{n}_\alpha^2 \rangle - \langle \hat{n}_\alpha \rangle^2$. The coherent state generates Poissonian number statistics and these fluctuations are large $\Delta^2(n_\alpha) = n$ in the superfluid state $J \gg U/n$, whereas they vanish deep in the Mott state (10).

Because the Hamiltonian (8) cannot be diagonalized analytically, some approximations are necessary for deriving explicit results [9, 10]. Here, we assume a large filling $n \gg 1$, which facilitates an expansion into (inverse) powers of n via $\hat{n}_\alpha = n + \delta\hat{n}_\alpha + \mathcal{O}(n^0)$ where the fluctuations $\delta\hat{n}_\alpha = \mathcal{O}(\sqrt{n})$ can be treated analytically. These fluctuations correspond to the Goldstone modes mentioned earlier and their propagation speed (in the continuum limit) can be estimated via $c^2 = \ell^2 J U n$, where ℓ is the lattice spacing. Thus, if J decreases fast enough, we get a horizon analogue as discussed in Sec. III.

Let us study a few examples for the temporal behavior of the sweep: For an exponentially decaying hopping rate $J(t) = J_0 \exp\{-\gamma t\}$, a horizon emerges for all values of γ and hence the Goldstone modes freeze, cf. Sec. III. The frozen number fluctuations are given by

$$\Delta^2(n_\alpha) = \langle \hat{n}_\alpha^2 \rangle - \langle \hat{n}_\alpha \rangle^2 = \langle \delta\hat{n}_\alpha^2 \rangle = n \frac{1 - e^{-2\pi\nu}}{2\pi\nu}, \quad (11)$$

where the adiabaticity parameter $\nu = U n / \gamma = \mu / \gamma$ is given by the ratio of the internal time scale (chemical potential $\mu = U n$) over the external sweep rate γ and thus measures the rapidity of the sweep. In agreement with the previous arguments, we recover the limiting cases $\Delta^2(n_\alpha) \uparrow n$ for $\nu \downarrow 0$ and $\Delta^2(n_\alpha) \downarrow 0$ for $\nu \uparrow \infty$. If the hopping rate merely exhibits a slow polynomial decay $J(t) \propto t^{-x}$ with $x < 2$, no horizon emerges and the number fluctuations do not freeze at a finite time but oscillate forever. The boundary case $J(t) \propto t^{-2}$ is quite interesting: Since it marks the limit for horizon formation, the modes show a behavior in between freezing at a finite value and eternal oscillation, i.e., they decay down to zero quite rapidly. This situation is analogous to a damped harmonic oscillator, where the critical damping [corresponding to $J(t) \propto t^{-2}$] marks the border between the over-damped (horizon formation and freezing) and the under-damped case (eternal oscillation). Hence this sweep dynamics $J(t) \propto t^{-2}$ would be the optimal choice for approaching the Mott state with $\Delta^2(n_\alpha) \downarrow 0$ most quickly [9, 10].

VI. EXTENDED BOSE-HUBBARD MODEL

If we extend the Hamiltonian (8) and include inter-site interactions given by $V_{\alpha\beta}$

$$\hat{H} = \sum_{\alpha\beta} (T_{\alpha\beta} \hat{a}_\alpha^\dagger \hat{a}_\beta + V_{\alpha\beta} \hat{n}_\alpha \hat{n}_\beta), \quad (12)$$

the phase diagram becomes much richer and now includes supersolid states etc. The superfluid-supersolid phase transition is a nice example for the scenario in Fig. 6 where the dispersion relation develops a “roton” dip which touches the vertical axis at the critical point (at zero temperature, cf. [11]). This implies an instability towards density modulations at a critical wavenumber k_{crit} , which corresponds to the period of the supersolid order parameter. As before, the modes become arbitrarily soft when approaching the transition – which entails interesting non-equilibrium effects. For example, in the presence of an external phase gradient (i.e., condensate flow), the branch of the “roton” dip corresponding to quasiparticles propagating against the condensate flow is closer to the axis, i.e., softer, than the other branch. Hence, approaching the transition too fast will create non-adiabatic excitations, which are stronger for these (softer) modes, because their gap is smaller, cf. Eq. (1). As a result, non-equilibrium phenomena may induce a current (stemming from the amplified quantum fluctuations) in the *opposite* direction – which might even compensate the condensate flow [11].

VII. SPINOR ($S = 1$) CONDENSATE

As an example for the behavior sketched in Figs. 5 and 7, let us consider a three-component Bose-Einstein condensate, which can be represented by an effective spinor field operator $\hat{\Psi} = (\hat{\Psi}_x, \hat{\Psi}_y, \hat{\Psi}_z)$ and the Hamiltonian density [12]

$$\begin{aligned} \hat{\mathcal{H}} = & \hat{\Psi}^\dagger \cdot \left(-\frac{\nabla^2}{2m} + \frac{c_0}{2} \hat{\Psi}^\dagger \cdot \hat{\Psi} \right) \hat{\Psi} \\ & - \frac{c_2}{2} (\hat{\Psi}^\dagger \times \hat{\Psi})^2 - q \hat{\Psi}_z^\dagger \hat{\Psi}_z. \end{aligned} \quad (13)$$

The first term is the same as in the case of one or two components (2) and contains the pseudo-spin independent kinetic term $\nabla^2/(2m)$ and coupling c_0 . The second term c_2 corresponds to spin-1 scattering channel and favors the ferromagnetic phase with maximum magnetization $\underline{F} = i(\hat{\Psi}^\dagger \times \hat{\Psi}) \neq 0$ due to $c_2 < 0$. Finally, the third term $q > 0$ denotes the quadratic Zeeman shift and would be minimized by placing all particles in the z -component, i.e., it favors the paramagnetic state $\langle \hat{\Psi}^\dagger \times \hat{\Psi} \rangle = 0$. The (second-order) phase transition separating the two regimes occurs at the critical point $q_{\text{crit}} = 2|c_2|\rho$.

Motivated by a recent experiment [13], we study the sweep from the paramagnetic to the ferromagnetic phase, cf. Fig. 9. Initially, the system stays in the potential minimum at zero magnetization, but after the quench, the initial minimum at $\underline{F} = 0$ turns to a local maximum and the system starts to roll down the potential hill, cf. Fig. 9. Since this is a symmetry-breaking phase transition, the direction of descent can be arbitrary and is set by the initial quantum (or thermal) fluctuations. Thus the spontaneously formed (measurable) directions of the magnetization \underline{F} provide a direct indicator for the initial quantum fluctuations, which were strongly amplified in that process. One result of these amplified quantum fluctuations could be the creation of topological defects (which cor-

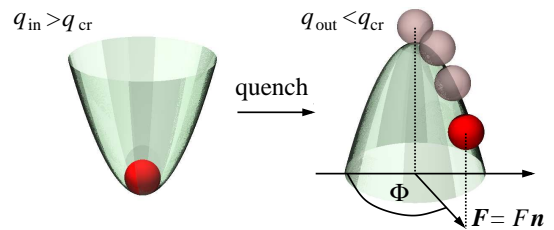


FIG. 9: Sketch of the energy landscape associated to Eq. (13). Initially, the system stays at $\underline{F} = 0$ (paramagnetic phase). After the transition, it starts to roll down the potential hill in some direction [$O(2)$ symmetry] which is set by the initial quantum (or thermal) fluctuations.

responds to the re-heating process mentioned in Sec. II) in a quantum analogue of the Kibble-Zurek [14, 15] mechanism, see also [3–5].

Since the $O(2)$ invariance of the Hamiltonian (13) with respect to rotations in the x, y -plane is broken by the ferromagnetic state, this phase supports topological (point) defects in the form of spin vortices in two spatial dimensions[29]. Such a defect corresponds to a spin configuration which cannot be deformed to a constant magnetization in a smooth way: Going around a vortex in a circle in real space, the magnetization describes a circle in the internal space of the ferromagnetic ground-state manifold, i.e., the magnetization always points towards the defect (vortex) or away from it (anti-vortex). The number of vortices (minus the number of anti-vortices) within a given area is the winding number \mathfrak{N} . Calculating this winding number for a circle of radius R , we obtain (for large R) the scaling law [12]

$$\langle \mathfrak{N}^2 \rangle \sim R \ln R, \quad (14)$$

which lies in between the random phase walk model (predicting $\langle \mathfrak{N}^2 \rangle \sim R$) and the random vortex gas model (predicting $\langle \mathfrak{N}^2 \rangle \sim R^2$) frequently discussed in the literature.

VIII. FINITE-SIZE SCALING

So far, our studies were devoted to the thermodynamic limit of infinitely large systems (cf. the footnote in Sec. V). Strictly speaking, phase transitions are well-defined in this limit only. For systems of finite size, the sharp transition at a precisely localizable critical point is typically broadened. Similarly, exact level crossings in the thermodynamic limit (as in Fig. 1) usually become avoided level crossings for finite systems since boundary terms and finite-size effects lift the degeneracy in general. As a result, the response time may not diverge at the critical point but remain bounded (even though very large). In order to study non-equilibrium phenomena, the scaling of the response time (or the energy gaps) with system size is very important.

As it turns out, this scaling may crucially depend on the order of the phase transition: For a typical first order transition (cf. Fig. 4), we have two competing ground states $|\psi_{<}\rangle$

and $|\psi_{>}\rangle$ which are locally distinguishable and become energetically favorable just before $|\psi_{<}\rangle = |\psi_0(g < g_{\text{crit}})\rangle$ and after $|\psi_{>}\rangle = |\psi_0(g > g_{\text{crit}})\rangle$ the transition. Due to their local distinguishability, their overlap decreases exponentially $\langle\psi_{<}|\psi_{>}\rangle \sim \exp\{-\mathcal{O}(n)\}$ with system size n (e.g., number of lattice sites or spins). In the low-energy sub-space spanned by $|\psi_{<}\rangle$ and $|\psi_{>}\rangle$, we have four relevant matrix elements of the Hamiltonian. At the critical point $g = g_{\text{crit}}$, the diagonal elements coincide $\langle\psi_{<}|H|\psi_{<}\rangle = \langle\psi_{>}|H|\psi_{>}\rangle$, but the off-diagonal matrix elements $\langle\psi_{<}|H|\psi_{>}\rangle = (\langle\psi_{>}|H|\psi_{<}\rangle)^*$ lead to an avoided level crossing with the fundamental gap $E_1 - E_0 = |\langle\psi_{<}|H|\psi_{>}\rangle|$. For a local Hamiltonian containing interactions of a limited number of sites (e.g., nearest neighbors) only $H \sim \text{poly}(n)$, the off-diagonal matrix elements scale exponentially $\langle\psi_{<}|H|\psi_{>}\rangle \sim \exp\{-\mathcal{O}(n)\}$ and hence the same scaling applies to the fundamental gap $E_1 - E_0 \sim \exp\{-\mathcal{O}(n)\}$. This result nicely matches the intuitive picture based on the energy landscape in Fig. 4. In order to stay in the ground state, the system has to tunnel through the energy barrier at the critical point. Since one would expect the height of the potential barrier to scale linearly with system size, the tunneling (i.e., response) time $\sim 1/(E_1 - E_0)$ should increase exponentially [17].

For transitions of second or higher order, on the other hand, such a tunnelling barrier is absent and there are no locally distinct competing ground states at the critical point. Hence there is no reason for an exponential scaling of the response time in this situation. Indeed, for several analytically solvable examples such as the quantum Ising model in a transverse field, the response time is found to scale polynomially (instead of exponentially) with system size [30]. Furthermore, the ground state changes less abruptly in second-order transitions than in those of first order, which also suggests that it should be easier to stay in the ground state.

IX. ADIABATIC QUANTUM ALGORITHMS

The intuition developed by considering the physics examples above might also be useful for gaining a deeper understanding in a rather different subject – quantum algorithms. Since the pioneering work of Shor and others, see, e.g., [18, 19], it is known that quantum computers (which operate in the full Hilbert space of all quantum states) should be able to solve certain problems much faster than all (known) classical algorithms. However, actually constructing a quantum computer of sufficient size is extremely hard since the fragile superpositions necessary for operating the quantum algorithm are very vulnerable to decoherence caused by the inevitable coupling to the environment. There are several ideas to overcome this problem: quantum error correcting codes, measurement-based (“one-way”) quantum computers, noise-resistant (e.g., topological) qubit realizations etc. In the following, we shall consider an alternative idea: adiabatic quantum algorithms [20]. In this scheme, the solution to a given problem is encoded into the ground state of an appropriately constructed problem Hamiltonian H_{out} . In order to arrive at the desired ground state of H_{out} , one starts with an initial

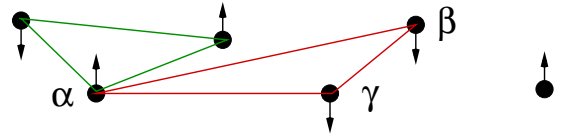


FIG. 10: Interaction topology of the Hamiltonian (16) where each triple (α, β, γ) corresponds to a triangle whose bonds govern the anti-ferromagnetic interaction $M_{\alpha, \beta}$.

Hamiltonian H_{in} , whose ground state is known and can be prepared easily, and then slowly transform it to the final problem Hamiltonian H_{out} , e.g., via a linear interpolation

$$H(t) = [1 - g(t)]H_{\text{in}} + g(t)H_{\text{out}}. \quad (15)$$

If this interpolation is slow enough, we end up in (or near) the final ground state encoding the solution to our problem [21]. The computational complexity manifests itself in the runtime T , which is bounded from below by the response time determined by the minimum gap. Now, for non-trivial problem Hamiltonians H_{out} , there is typically a critical point where the fundamental gap $E_1 - E_0$ between the ground state and the first excited state becomes very small – which bears strong similarities to a quantum phase transition, see also [22].

Let us study an explicit example. A rather interesting class of problems is *exact cover-3*, which corresponds to the following requirement: Given a set of triples $(\alpha, \beta, \gamma) \in \mathbb{N}^3$, find at least one bit-string $z_\alpha \in \{0, 1\}$ which satisfies the constraint $z_\alpha + z_\beta + z_\gamma = 1$ for all triples (α, β, γ) . It can be shown that other tasks such as factoring can be mapped onto this problem class. A suitable problem Hamiltonian is given by the sum of $(\sigma_\alpha^z + \sigma_\beta^z + \sigma_\gamma^z + 1)^2$ over all these triples, which yields

$$H_{\text{out}} = \sum_{\alpha, \beta=1}^n M_{\alpha, \beta} \sigma_\alpha^z \sigma_\beta^z + 2 \sum_{\alpha=1}^n N_\alpha \sigma_\alpha^z + \text{const}. \quad (16)$$

This corresponds to a frustrated anti-ferromagnet in an external field N_α , where the interaction topology $M_{\alpha, \beta}$ is determined by the set of triples, cf. Fig. 10.

Now, given the final problem Hamiltonian H_{out} above, what could be a suitable initial Hamiltonian H_{in} ? Obviously, H_{in} should not be diagonal in the σ_α^z -basis – in this case, we would have exact (instead of avoided) level crossings and an adiabatic evolution would be impossible. Therefore, most previous studies (see, e.g., [20]) adopted the form

$$H_{\text{in}} = \sum_{\alpha} L_\alpha \sigma_\alpha^x. \quad (17)$$

On the other hand, inspired by the findings in Sec. VIII, one could try to choose H_{in} in a way such that the change from H_{in} to H_{out} is similar to a second-order phase transition. The observation that symmetry-breaking/restoring phase transitions are often (though not always) of second order indicates one idea for doing this. An apparent symmetry of H_{out} is its $O(2)$ invariance under rotations around the z -axis generated by

$$\Sigma^z = \sum_{\alpha=1}^n \sigma_\alpha^z. \quad (18)$$

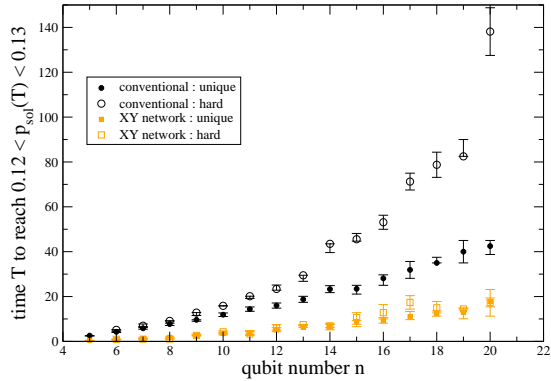


FIG. 11: Plot of the runtime necessary for an adiabatic evolution for the conventional scheme (17) and the XY network in Eqs. (16) and (19). The hollow symbols correspond to especially hard problems within the class *exact cover-3*.

Now, if we start with the ferromagnetic Hamiltonian

$$H_{\text{in}} = - \sum_{\alpha, \beta=1}^n M_{\alpha, \beta} (\sigma_{\alpha}^x \sigma_{\beta}^x + \sigma_{\alpha}^y \sigma_{\beta}^y), \quad (19)$$

which is also $O(2)$ invariant, but whose degenerated ground states break this symmetry, one would expect that the resulting adiabatic quantum algorithm is very similar to a second-order phase transition, where the system finds it easier to stay in the ground state. In this way, physics intuition motivates a new way of constructing quantum algorithms [17]. Indeed, numerical simulations suggest that the algorithm described in Eqs. (16) and (19) is superior (in average) to the conventional scheme (17), cf. Fig. 11.

X. DECOHERENCE

One of the (original) motivations for adiabatic quantum computing was the robustness of the ground state against de-

cay and dephasing errors. However, this does not imply that these algorithms are completely free of decoherence: A finite temperature environment may heat up the system and cause excitations, which would result in computational errors (since the ground state, not an excited state, encodes the solution to our problem). Furthermore, non-equilibrium phenomena may also cause excitations at zero temperature due to the coupling to an environment. Since the energy gap typically becomes very small at some point of the interpolation, the algorithm will be very vulnerable near this point. Of course, the same applies to the critical point in more general quantum phase transitions. For an adiabatic version [23] of the Grover [19] quantum search algorithm – which corresponds to a first-order transition – we found that the induced excitation probability strongly depends on the spectral function $f_{\text{bath}}(\omega)$ of the environment and scales as [24]

$$P_{\text{error}} \sim \frac{f_{\text{bath}}(\Delta E_{\text{min}})}{\Delta E_{\text{min}}}, \quad (20)$$

where ΔE_{min} is the minimum energy gap. Hence, if $f_{\text{bath}}(\omega)$ vanishes fast enough in the infrared $\omega \rightarrow 0$, the error rate can be kept under control. However, repeating the same analysis for the Ising model [25] and the sweep through the second-order phase transition, we find that the excitation probability increases with system size n , independently of $f_{\text{bath}}(\omega)$. This suggests that second-order transitions are more suitable for adiabatic quantum computing – but, at the same time, more vulnerable to decoherence (which requires some error correction techniques).

Acknowledgments

This work was supported by the Emmy-Noether Programme of the German Research Foundation (DFG) under grant # SCHU 1557/1-2,3.

-
- [1] M. Born and V. A. Fock, *Beweis des Adiabatenatzes*, Zeitschrift für Physik A **51**, 165 (1928).
 - [2] S. Sachdev, *Quantum Phase transitions*, (Cambridge University Press, Cambridge, UK, 1999).
 - [3] W. H. Zurek, U. Dorner, and P. Zoller, *Dynamics of a Quantum Phase Transition*, Phys. Rev. Lett. **95**, 105701 (2005).
 - [4] J. Dziarmaga, *Dynamics of a quantum phase transition: Exact solution of the quantum Ising model* Phys. Rev. Lett. **95**, 245701 (2005).
 - [5] B. Damski, *The Simplest Quantum Model Supporting the Kibble-Zurek Mechanism of Topological Defect Production: Landau-Zener Transitions from a New Perspective*, Phys. Rev. Lett. **95**, 035701 (2005).
 - [6] U. R. Fischer and R. Schützhold, *Quantum simulation of cosmic inflation in two-component Bose-Einstein condensates*, Phys. Rev. A **70**, 063615 (2004).
 - [7] R. Schützhold, *Dynamical zero-temperature phase transitions and cosmic inflation/deflation*, Phys. Rev. Lett. **95**, 135703 (2005).
 - [8] R. Schützhold, *Emergent horizons in the laboratory*, Class. Quantum Grav. **25**, 114011 (2008).
 - [9] R. Schützhold, M. Uhlmann, Y. Xu and U. R. Fischer, *Sweeping from the superfluid to Mott phase in the Bose-Hubbard model*, Phys. Rev. Lett. **97**, 200601 (2006).
 - [10] U. R. Fischer, R. Schützhold, and M. Uhlmann, *Bogoliubov theory of quantum correlations in the time-dependent Bose-Hubbard model*, Phys. Rev. A **77**, 043615 (2008).
 - [11] R. Schützhold, M. Uhlmann, and U. R. Fischer, *Effects of fluctuation*

- tuations in the superfluid-supersolid phase transition on the lattice*, arXiv:0804.1686.
- [12] M. Uhlmann, R. Schützhold, and U. R. Fischer, *Vortex quantum creation and winding number scaling in a quenched spinor Bose gas*, Phys. Rev. Lett. **99**, 120407 (2007).
- [13] L. E. Sadler, J. M. Higbie, S. R. Leslie, M. Vengalattore, and D. M. Stamper-Kurn, *Spontaneous symmetry breaking in a quenched ferromagnetic spinor Bose condensate*, Nature **443**, 312 (2006).
- [14] T. W. B. Kibble, *Topology of cosmic domains and strings*, J. Phys. A **9**, 1387 (1976).
- [15] W. H. Zurek, *Cosmological experiments in superfluid helium?*, Nature (London) **317**, 505 (1985).
- [16] P. Laguna and W. H. Zurek, *Density of Kinks after a Quench: When Symmetry Breaks, How Big are the Pieces?*, Phys. Rev. Lett. **78**, 2519 (1997).
- [17] R. Schützhold and G. Schaller, *Adiabatic quantum algorithms as quantum phase transitions: first versus second order*, Phys. Rev. A **74**, rapid commun. 060304 (2006).
- [18] P. W. Shor, *Polynomial-Time Algorithms for Prime Factorization and Discrete Logarithms on Quantum Computer*, SIAM J. Comp. **26**, 1484 (1997).
- [19] L. K. Grover, *Quantum Mechanics Helps in Searching for a Needle in a Haystack*, Phys. Rev. Lett. **79**, 325 (1997).
- [20] E. Farhi *et al.*, *A Quantum Adiabatic Evolution Algorithm Applied to Random Instances of an NP-Complete Problem*, Science **292**, 472 (2001).
- [21] R. Schützhold, S. Mostame, and G. Schaller, *General error estimate for adiabatic quantum computing*, Phys. Rev. A **73**, 062307 (2006).
- [22] J. I. Latorre and R. Orús, *Adiabatic quantum computation and quantum phase transitions*, Phys. Rev. A **69**, 062302 (2004).
- [23] J. Roland and N. J. Cerf, *Quantum search by local adiabatic evolution*, Phys. Rev. A **65**, 042308 (2002).
- [24] M. Tiersch and R. Schützhold, *Non-Markovian decoherence in the adiabatic quantum search algorithm*, Phys. Rev. A **75**, 062313 (2007).
- [25] S. Mostame, G. Schaller, and R. Schützhold, *Decoherence in a dynamical quantum phase transition of the Ising chain*, Phys. Rev. A **76**, rapid commun. 030304 (2007).
- [26] A counter-example would be a phase gradient and thus flow through our sample, cf. Sec. VI
- [27] The initial state should not be important as the system is supposed to be adiabatic initially.
- [28] Strictly speaking, there is no Bose-Einstein condensation and thus also no phase transition in a one-dimensional homogeneous lattice of infinite length. Therefore, we should consider either lattices of two or more spatial dimensions or chains of sufficiently small length. In the latter case, however, there is no sharp phase transition but only an approximate one (cf. Sec. VIII).
- [29] In three spatial dimensions, point defects would not be possible for a broken $O(2) \simeq S_1$, but only line defects. For a broken $SO(3)$, on the other hand, point defects would exist in three spatial dimensions due to $SO(3)/O(2) \simeq S_2$.
- [30] However, the absence of the sketched reason for an exponential scaling does not necessarily imply that the minimum fundamental gap ($E_1 - E_0$) must scale polynomially for all second-order transitions (as a counter-example, consider the random Ising chain).